

## Light-controlled anchoring of meandering spiral waves

O. Steinbock and S. C. Müller

*Max-Planck-Institut für Molekulare Physiologie, Rheinlanddamm 201, D-4600 Dortmund 1, Germany*

(Received 11 November 1992)

Meandering spiral waves in the light-sensitive excitable Belousov-Zhabotinsky reaction with tips proceeding along epicycles were forced to rigid rotation. This spiral anchoring was induced by an argon laser beam creating an unexcitable disk close to the tip. The stabilized spirals rotate with frequencies above the low secondary frequency of meandering. Simulations using a simple reaction-diffusion model demonstrate that anchoring is only possible up to a critical radius of the disk. For this critical value anchored spirals obey the unstable primary parameters (radius and frequency) of compound motion.

PACS number(s): 05.70.Ln, 82.20.Mj, 82.20.Wt, 87.90.+y

Rotating spiral waves are intensively studied in different excitable media, for instance the aggregating *Dictyostelium amoebas* [1], the CO oxidation on platinum [2], cardiac muscles [3], and chemical reactions [4,5]. In the well-known Belousov-Zhabotinsky (BZ) reaction [6], spiral waves reveal unexpected dynamical features of tip motion [7]. Depending on the chemical composition, rigid rotation around fixed circular cores [5], compound tip motion [8–10], or even irregular “hypermeandering” [7,11] are observed. Compound (meandering) traces of the tips exhibit quasiperiodicity and can be approximated by epicycles [9] generated by superposing two circular motions having distinctively different radii ( $r_1, r_2$ ) and frequencies ( $f_1, f_2$ ). The Cartesian coordinates of these tip trajectories are represented by

$$\begin{aligned} x(t) &= r_1 \cos(2\pi f_1 t + \alpha) + r_2 \cos(2\pi f_2 t + \beta), \\ y(t) &= r_1 \sin(2\pi f_1 t + \alpha) - r_2 \sin(2\pi f_2 t + \beta). \end{aligned} \quad (1)$$

In this work we demonstrate that circular obstacles can anchor meandering spirals to strictly periodic motion. We investigate the limits of frequencies  $f_A$  and radii  $r_A$  for spiral anchoring and compare these values to the corresponding parameters of compound tip motion  $f_i, r_i$  ( $i = 1, 2$ ). Furthermore, we study the release of anchored tips after the obstacle has been removed. The validity of the observed phenomena is corroborated by numerical integration of a simple reaction-diffusion model.

The experiments were performed in a light-sensitive variant of the BZ reaction, allowing an efficient control of excitability [12,13]. The used catalyst ruthenium-bipyridyl promotes the autocatalytic production of the propagator species  $\text{HBrO}_2$  only in its reduced and electronically unexcited state [14]. A strongly illuminated spot can serve as the anchoring obstacle. Once the ruthenium complex is photochemically excited, it slowly catalyzes the production of the inhibitor bromide. 4 mM  $\text{Ru}(\text{bpy})_3^{2+}$  was immobilized in a silica-gel matrix to avoid hydrodynamic perturbations [15]. The reaction starts slowly after pouring an equal volume of BZ solution on top of the gel layer. After diffusive equilibration ( $\approx 5$  min) the reactant concentrations in the layer are

0.13M NaBr, 0.37M  $\text{NaBrO}_3$ , 0.33M malonic acid, and 0.53M  $\text{H}_2\text{SO}_4$  (for these values the bromination of malonic acid was not taken into account). The temperature was kept fixed at  $(23 \pm 1)^\circ\text{C}$ . The dynamic two-dimensional (2D) transmission (stabilized high-pressure mercury lamp; 490 nm) of the distributed medium was detected by a charge-coupled-device camera (Hamamatsu C3077) and stored on a video recorder. Single images and movies were digitized by a data acquisition card (Data Translation, DT-2851,  $512 \times 512$  pixel, 8 bits gray level) and saved on a PC hard disk for further computational analysis. An argon laser (514-nm line; 0.8 W; attenuated by a neutral density filter whose optical density was 2.0) was used to create the unexcitable, nearly circular spot (diameter 0.4 mm; almost rectangular intensity profile) in the gel layer, which serves as the desired spiral anchor. The optical equipment (lamp and laser) was kept fixed, while the dish containing the gelled BZ system was movable (details in Ref. [12]).

In the described chemical medium spiral waves exist for more than four hours. During most of this period spiral tips move along unclosed four-leaved trajectories. The size of this meander pattern increases slowly with the aging of the solution. In the presented analyses tip positions were obtained visually, supported by computational image processing: After a small gray-level interval was transformed to a pseudocolor, a digital reticle was shifted to the location of highest curvature of the tip contour. These pixel coordinates were stored on a PC hard disk for further analysis. Figure 1(a) shows the 2D transmission of a spiral pattern with the superposed path of its tip (white curve), obtained for a 207-s time interval during which 75 tip positions were detected and connected by cubic spline interpolation. The existence of a tip anchoring effect is demonstrated in Fig. 1(b), showing a logical overlay (maximum value) of eight consecutive digital snapshots of one spiral, now rotating around a circular laser spot. The previous compound tip motion is stabilized to simple rotation along the boundary of the unexcitable disk. Larger spots allow the anchoring of spirals, as well, but increase the rotation period (in this example  $T = 59$  s). When realizing smaller spots, scattering of light in the gel renders controlled experimentation

difficult.

Figure 2 shows the tip coordinates  $x$  and  $y$  as a function of time. The compound oscillations of  $x$  and  $y$  ( $t < 0$  s) change to simple harmonic ones, when the laser is switched on ( $t = 0$  s). The details of the initial capture of the meandering tip depend on the phase of its motion and the relative location of the laser spot, which has to be positioned in the domain of the meander path. There is no evidence for a temporal limitation of this anchoring procedure during the entire period of spiral wave existence.

Fast Fourier transformation (FFT) of these temporal traces  $x(t)$  and  $y(t)$  results in the power spectra of Fig. 3. Figure 3(a) shows the power spectral density for the unperturbed compound tip motion. It is clearly dominated by two peaks around frequencies  $f_1 = 0.0232$  Hz and  $f_2 = 0.0089$  Hz. The corresponding ratio  $f_1/f_2 = 2.58$  is in good agreement with the observation of an unclosed four-leaved tip orbit [see Fig. 1(a)]. According to Eqs. (1)

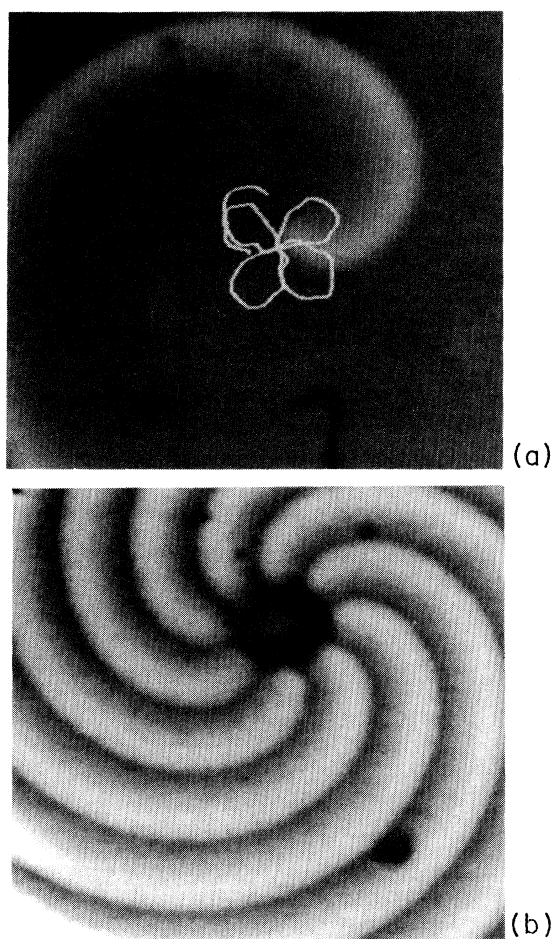


FIG. 1. (a) Digital snapshot of a spiral wave in the ruthenium-catalyzed Belousov-Zhabotinsky reaction observed at 490 nm. The superposed white curve indicates the trace of the unperturbed spiral tip. Image area  $2.8 \times 2.8 \text{ mm}^2$ . (b) Logical overlay of eight images with a spiral tip anchored by an unexcitable disk (laser spot, diameter 0.4 mm). The tip motion is changed from compound (a) to simple rotation. Time interval between consecutive images: 7.45 s.

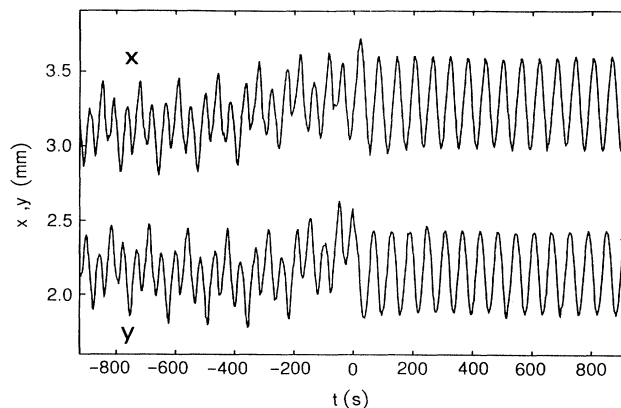


FIG. 2.  $x$  and  $y$  coordinates of the spiral tip as a function of time. Each curve is composed of 670 values, corresponding to a sample interval of 2.76 s. Up to  $t = 0$  s the tip is meandering and traversing the flowerlike path shown in Fig. 1(a). At  $t = 0$  s the laser is switched on and the resulting unexcitable laser spot region anchors the tip to simple rotation.

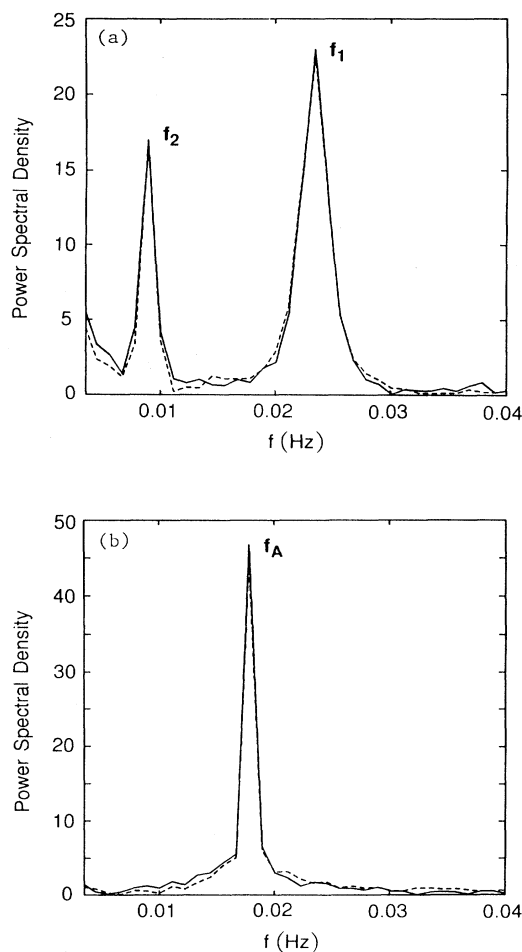


FIG. 3. Power spectra of the data given in Fig. 2: (a) Meandering state ( $-925 \text{ s} < t < -31 \text{ s}$ ), (b) anchored state ( $27 \text{ s} < t < 922 \text{ s}$ ). Spectrum (a) has two clearly separated peaks at  $f_1 = 0.0232$  Hz and  $f_2 = 0.0089$  Hz, while the anchored tip motion shows only one frequency  $f_A = 0.0178$  Hz. Spectra of  $x(t)$  and  $y(t)$  are plotted as solid and dashed lines, respectively.

a closed four-leaved orbit must have a frequency ratio of 3. The power spectrum of Fig. 3(b) describes the anchored state with a single maximum at  $f_A=0.0178$  Hz and proves the existence of a forced transition from compound motion to simple rotation. The period of anchored rotation is 13 s larger than the period  $1/f_1$  of the meandering spiral, but 56 s shorter than  $1/f_2$ . We found no significant differences between the spectra of  $x(t)$  and  $y(t)$ , respectively. A biharmonic least-squares fit of  $y(t)$  yields the radii  $r_1=0.11$  mm,  $r_2=0.18$  mm, and  $r_A=0.28$  mm. Furthermore, we studied the release of the tip, when the laser is switched off and the anchor is thus removed. Figure 4 shows the almost circular path of the tip until the end of external stabilization (open arrow) and its subsequent motion after release. After the stabilization of the orbit during anchoring is lost, the former meandering process comes to life again. Hence, the system shows no memory effect.

To achieve a better understanding of the observed processes we performed computer simulations using the following simple reaction-diffusion model [16,17] for the propagator  $u$  and the controller  $v$  species:

$$\frac{\partial u}{\partial t} = D_u \Delta u + \frac{1}{\epsilon} u(1-u) \left[ u - \frac{v+b}{a} \right], \quad (2)$$

$$\frac{\partial v}{\partial t} = u - v, \quad (3)$$

with the diffusion coefficient  $D_u=1.0$ , the parameters  $a=0.5$ ,  $b=0.03$ , and  $\epsilon=\frac{1}{130}$ . By integrating this system of partial differential equations on a square domain of  $256 \times 256$  grid points (with a length of  $L=22$  and  $dt=1.489 \times 10^{-3}$ ) we were able to find meandering spiral waves with a frequency ratio of  $f_1/f_2=2.5$  and radii  $r_1=7.6$ ,  $r_2=11.8$  grid points. The trajectories of the

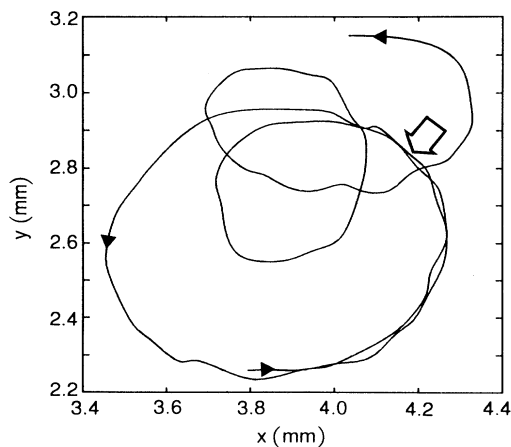


FIG. 4. Anchored spiral tip is released and starts to meander again, when the laser beam is switched off (open arrow). The depicted trajectory of this transition describes a newly formed floral pattern relative to the anchor region. The first loop is located inside the former laser spot area. In this typical experiment the laser was switched on for 240 s. Traversing the depicted path takes the spiral tip 232 s.

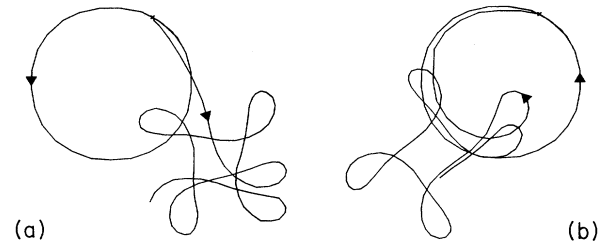


FIG. 5. Simulation of the experimentally observed spiral tip release (Fig. 4) by integration of a simple reaction-diffusion model. The anchor was realized by fixing the values of  $u$  (propagator) and  $v$  (controller) to  $(0.0,0.0)$  in (a) and  $(0.0,0.5)$  in (b). The good qualitative agreement between simulation (b) and the experiment can be explained by the production of the inhibitor bromide inside the laser illuminated disk area.

spiral tip were provided by the evolution of the intersection of the  $u=0.5 \pm 0.06$  and  $v=0.247 \pm 0.06$  level curves.

Figure 5 shows two examples of a tip which first rotates around an unexcitable disk (radius 15 grid points) and, after release, follows newly formed meandering orbits. Anchoring was performed by fixing the propagator  $u$  and controller  $v$  to specific values for all grid points inside the unexcitable anchor region. The trace in Fig. 5(a) was obtained by fixed values  $(u,v)=(0,0)$  inside this region, that of Fig. 5(b) by  $(u,v)=(0,0.5)$ . In graph (a) the tip path is rapidly reversed after release, describes a long drift away from the former anchor, and finally starts to meander. A similar behavior was found by adjusting parameter  $b$  to higher values (e.g.,  $b=0.12$ ), which corresponds to loss of excitability. On the other hand, in graph (b) the tip trajectory deviates smoothly from the circle determined by the former anchor and begins to

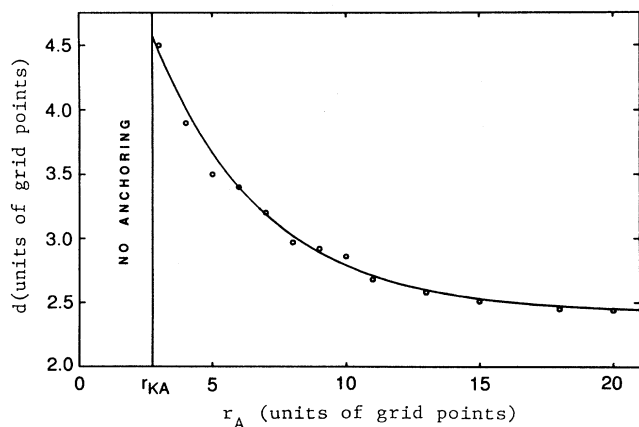


FIG. 6. Distance  $d$  between anchor boundary and tip as a function of anchor radius  $r_A$ . Resulting from simulations on an array of  $256 \times 256$  grid points (grid spacing  $h=0.0863$ ) the monotonic decay of  $d$  is approximated by an exponential function (solid line). Below a critical value  $r_{KA}$  the tip starts again to meander.

loop continuously. While both approaches for simulating the conditions in the experimental laser spot are successful in anchoring the spiral, the scenario in Fig. 5(b) reproduces the experiment more closely than that of Fig. 5(a). Probably, this result gives a clue for the production of the inhibitor bromide inside the laser spot: The state  $(u,v)=(0,0.5)$  is located in the refractory zone of the phase plane, whereas  $(u,v)=(0,0)$  is excitable. Hence,  $(u,v)=(0,0.5)$  simulates the inhibitor-enriched laser spot better than the other completely recovered one.

The numerical simulations yield the existence of a critical minimal anchor radius  $r_{KA}$  (approximately 3 grid points). For obstacles smaller than  $r_{KA}$  anchoring is not possible and the tip resumes meandering. The rotation frequency  $f_A$  for a spiral anchored near  $r_{KA}$  is very close to the high frequency  $f_1$  of unperturbed meandering. Furthermore, the radius of the tip orbit is equal to  $r_1$  when the anchor radius reaches  $r_{KA}$ . Figure 6 shows that the distance  $d$  between anchor boundary and tip orbit decays monotonically for increasing values of  $r_A$ . This de-

cay can be approximated by an exponential function. The mechanism for this repulsion effect is not yet clearly understood. One possible explanation is that an increase of the orbit frequency  $f_A$  leads to a reduced excitability close to the tip which causes the observed repulsion.

Our results demonstrate that an excitable medium in which unperturbed spiral tips describe epicyclelike trajectories also can support rigid rotation with frequencies up to the high primary frequency of meandering. This elucidates the nature of meandering from a different point of view: unexcitable disks can remove the instability of tip motion and establish circular orbits close to the size of the small unstable lobes of compound motion. Furthermore, the presented investigations give insights into the phenomenon of uncontrolled anchoring, as recently observed in inhomogeneous cardiac muscle [18].

We thank Zs. Nagy-Ungvarai and V. S. Zykov for discussions and I. Beyer for technical assistance.

- 
- [1] G. Gerisch, *Naturwissenschaften* **58**, 430 (1971).
  - [2] S. Jakubith, H. H. Rotermund, W. Engel, A. von Oertzen, and G. Ertl, *Phys. Rev. Lett.* **65**, 3013 (1990).
  - [3] J. M. Davidenko, P. Kent, and J. Jalife, *Physica D* **49**, 182 (1991).
  - [4] A. T. Winfree, *Science* **175**, 634 (1972).
  - [5] S. C. Müller, Th. Plesser, and B. Hess, *Physica D* **24**, 87 (1987).
  - [6] *Oscillations and Travelling Waves in Chemical Systems*, edited by R. J. Field and M. Burger (Wiley, New York, 1985).
  - [7] Zs. Nagy-Ungvarai, J. Ungvarai, and S. C. Müller, *Chaos* (to be published).
  - [8] W. Jahnke, W. E. Skaggs, and A. T. Winfree, *J. Phys. Chem.* **93**, 740 (1989).
  - [9] G. S. Skinner and H. L. Swinney, *Physica D* **48**, 1 (1991).
  - [10] T. Plesser, S. C. Müller, and B. Hess, *J. Phys. Chem.* **94**, 7501 (1990).
  - [11] A. T. Winfree, *Chaos* **1**, 303 (1991).
  - [12] O. Steinbock and S. C. Müller, *Physica A* **188**, 61 (1992).
  - [13] K. I. Agladze, V. A. Davydov, and A. S. Mikhailov, *Pis'ma Zh. Eksp. Teor. Fiz.* **45**, 601 (1987) [*JETP Lett.* **45**, 767 (1987)].
  - [14] L. Kuhnert, *Naturwissenschaften* **73**, 96 (1986).
  - [15] T. Yamaguchi, L. Kuhnert, Zs. Nagy-Ungvarai, S. C. Müller, and B. Hess, *J. Phys. Chem.* **95**, 5831 (1991).
  - [16] D. Barkley, M. Kness, and L. S. Tuckerman, *Phys. Rev. A* **42**, 2489 (1990).
  - [17] D. Barkley, *Physica D* **49**, 61 (1991).
  - [18] J. M. Davidenko, A. V. Pertsov, R. Salomonsz, W. Baxter, and J. Jalife, *Nature* **355**, 349 (1992).

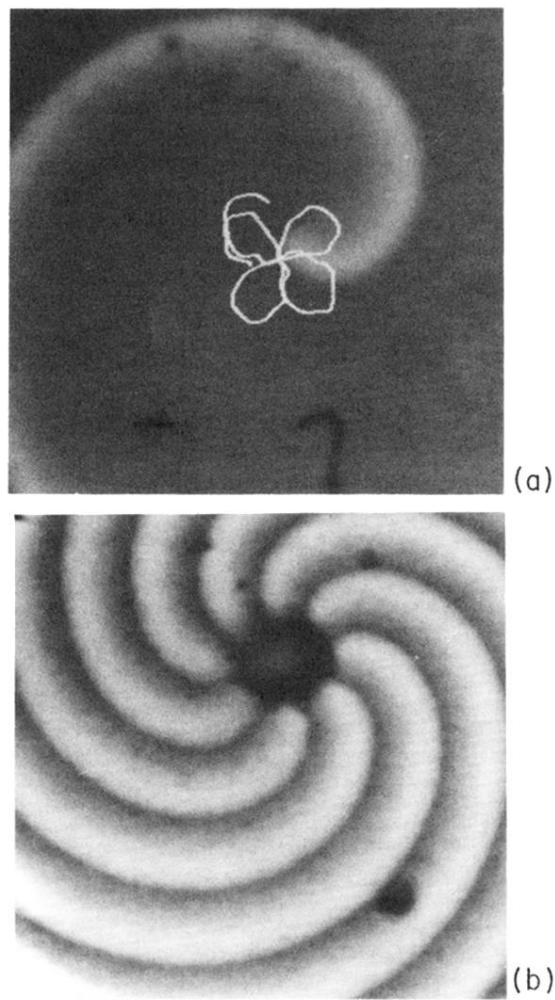


FIG. 1. (a) Digital snapshot of a spiral wave in the ruthenium-catalyzed Belousov-Zhabotinsky reaction observed at 490 nm. The superposed white curve indicates the trace of the unperturbed spiral tip. Image area  $2.8 \times 2.8 \text{ mm}^2$ . (b) Logical overlay of eight images with a spiral tip anchored by an unexcitable disk (laser spot, diameter 0.4 mm). The tip motion is changed from compound (a) to simple rotation. Time interval between consecutive images: 7.45 s.